

## Temperature dependence of electron spin relaxation in bulk GaN

J. H. Buß,<sup>1</sup> J. Rudolph,<sup>1</sup> F. Natali,<sup>2</sup> F. Semond,<sup>2</sup> and D. Hägele<sup>1</sup>

<sup>1</sup>*Arbeitsgruppe Spektroskopie der kondensierten Materie, Ruhr-Universität Bochum, Universitätsstraße 150, D-44780 Bochum, Germany*

<sup>2</sup>*Centre de Recherche sur l'Hétéro-Epitaxie et ses Applications, Centre National de la Recherche Scientifique, Rue Bernard Gregory, Sophia Antipolis, 06560 Valbonne, France*

(Received 29 January 2010; revised manuscript received 11 March 2010; published 30 April 2010)

The electron spin dynamics in *n*-type wurtzite GaN is studied by time-resolved Kerr rotation for temperatures from 80 to 295 K and magnetic fields up to 1 T. The temperature and magnetic field dependence of the spin-relaxation time are in good agreement with D'yakonov-Perel' theory. We present an analytic expression for the spin-relaxation tensor for semiconductors with wurtzite structure that also includes the interference of Rashba and Dresselhaus contributions.

DOI: 10.1103/PhysRevB.81.155216

PACS number(s): 78.47.D-, 72.25.Rb, 78.66.Fd

Spin phenomena in semiconductors have raised enormous interest in the last years, both from a fundamental point of view as well as for possible applications.<sup>1-3</sup> The central mechanism for spin-related effects in semiconductors is spin-orbit coupling (SOC). It allows for, e.g., the controlled manipulation of spins, but is at the same time also the main reason for spin relaxation in most of the III-V semiconductors, especially at elevated temperatures. Therefore, a thorough understanding of SOC is essential. For semiconductors with zinc-blende structure, and here in particular for GaAs, a detailed knowledge about SOC is already achieved.<sup>4,5</sup> In contrast, the knowledge about SOC in the emerging class of wide-gap semiconductors with wurtzite structure is still rudimentary. Among these materials, GaN is intensively studied. Besides its potential for optoelectronics<sup>6,7</sup> and for high-frequency and high-power electronics,<sup>8</sup> also its spin-related properties put GaN into the focus of intense research. Predictions of above room-temperature ferromagnetism in rare-earth- or transition-metal-doped GaN (Refs. 9 and 10) as well as the weak SOC as compared to, e.g., GaAs make GaN a promising material for spintronics. Also from a fundamental point of view, the investigation of SOC in wurtzite materials is highly interesting as the crystal structure and symmetry strongly influence SOC.

The main manifestation of SOC in GaN is a spin splitting of the bands due to the inversion asymmetry of the crystal lattice. This spin splitting, which acts like an effective magnetic field  $\mathbf{\Omega}(\mathbf{k})$  on the electron's spin, depends on the electron's momentum  $\mathbf{k}$  and is the basis for the D'yakonov-Perel' spin-relaxation mechanism.<sup>11</sup> The electron spin dynamics gives therefore insight into SOC in GaN. However, it has been studied only rarely in bulk wurtzite GaN,<sup>12,13</sup> and systematic studies for temperatures above 80 K are missing so far. Here, we investigate the electron spin dynamics and relaxation in bulk GaN by time-resolved Kerr rotation (TRKR) spectroscopy<sup>14,15</sup> in the temperature range from 80 to 295 K and external magnetic fields up to 1 T.

The samples studied are 2- $\mu\text{m}$ -thick GaN epilayers grown by molecular beam epitaxy on a 0.25  $\mu\text{m}$  AlN/0.25  $\mu\text{m}$  GaN stress mitigating layer on top of a 44 nm AlN nucleation layer on Si(111) substrates.<sup>16,17</sup> Sample A is Si *n*-doped with a doping level of  $2.2 \times 10^{17} \text{ cm}^{-3}$ , while sample B is intentionally undoped with a very low typical residual background doping of  $< 5 \times 10^{15} \text{ cm}^{-3}$ .

For the TRKR experiments, the output of a femtosecond mode-locked Ti:sapphire laser with a repetition rate of 80 MHz was frequency doubled by a beta barium borate crystal and split into pump and probe beam. The circularly polarized pump pulses were focused down to a spot with a diameter of about 60  $\mu\text{m}$  on the sample surface and created a spin-polarized electron ensemble. The temporal evolution of the spin polarization was followed via the Kerr rotation of the linearly polarized probe beam that was time delayed by a mechanical delay line and focused to the same spot as the pump beam. The energy of pump and probe pulses was varied from  $E=3.460 \text{ eV}$  at 80 K to  $E=3.404 \text{ eV}$  at 295 K to account for the temperature induced shift of the band gap. The average pump power was kept at 4 mW, corresponding to an estimated density of  $n_{\text{exc}}=1 \times 10^{16} \text{ cm}^{-3}$  photoexcited carriers, the probe beam power was 400  $\mu\text{W}$ . The samples were mounted in a cold-finger cryostat at temperatures between 80 and 295 K. An external magnetic field  $B_{\text{ext}}$  up to 1 T was applied in the sample plane.

Figure 1 shows TRKR transients for the *n*-doped sample A for temperatures from 80 to 295 K in a magnetic field  $B_{\text{ext}}=1.05 \text{ T}$ . The transients show a fast initial decay, an oscillatory behavior if an external magnetic field  $B_{\text{ext}}$  is applied, and a temporal decrease in the TRKR signal amplitude. These three features, that persist at all temperatures, will be addressed in the following.

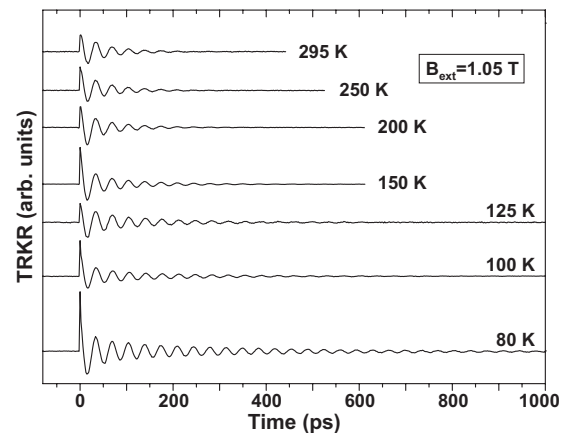


FIG. 1. TRKR transients for sample A in a magnetic field  $B_{\text{ext}}=1.05 \text{ T}$  and temperatures from 80 to 295 K.

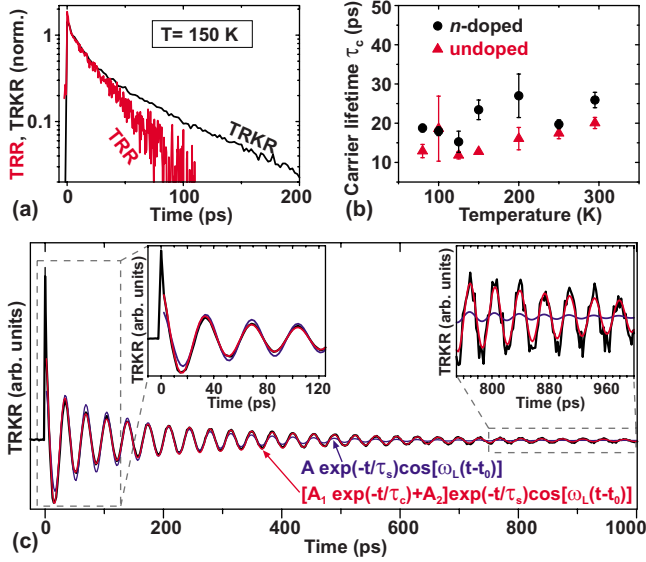


FIG. 2. (Color online) (a) TRR and TRKR transients for sample A at  $T=150$  K. (b) Temperature dependence of the carrier lifetime  $\tau_c$  of sample A (dots) and sample B (triangles). (c) TRKR transient (black line) of sample A at  $T=80$  K and  $B_{\text{ext}}=1.05$  T with fits by the function  $[A_1 \exp(-t/\tau_c)+A_2]\exp(-t/\tau_s)\cos[\omega_L(t-t_0)]$  (red line) and a damped cosine  $A \exp(-t/\tau_s)\cos[\omega_L(t-t_0)]$  (blue line). The insets show the time range from  $t=-10$  ps to 125 ps and from  $t=750$  ps to 1000 ps, respectively, in more detail.

The fast initial decay becomes highlighted by its steep slope in a semilog scale plot [black line in Fig. 2(a)], where it lasts up to  $\approx 35$  ps, before the decay slows down. This rapid initial decrease in the TRKR signal is caused by the decay of the carrier density as is demonstrated by the very good match between the TRKR signal and the time-resolved reflectivity (TRR) [red line in Fig. 2(a)] as a measure of the carrier density. A possible signature of the very fast excitonic spin relaxation, that occurs on a subpicosecond time scale in GaN,<sup>18,19</sup> is temporally not resolved in our measurements. A carrier lifetime  $\tau_c$  was extracted from a single exponential fit of the form  $A \exp(-t/\tau_c)$  to the TRR transients. The carrier lifetime is only weakly temperature dependent and for both samples always shorter than 27 ps [Fig. 2(b)]. Therefore, the TRKR signal at times later than  $t \approx 50$  ps is for the whole temperature range solely attributed to electrons in the conduction band, and we will concentrate on the electron spin dynamics at these later times in the following.

The TRKR signal oscillates with time if an external magnetic field  $B_{\text{ext}}$  is applied in the sample plane [cf. Fig. 1] with increasing oscillation frequency for increasing  $B_{\text{ext}}$ . These oscillations are caused by the Larmor precession of the electron spins around the external magnetic field with the Larmor precession frequency

$$\omega_L = g\mu_B B_{\text{ext}}/\hbar, \quad (1)$$

where  $\mu_B$  is the Bohr magneton and  $g$  the Landé  $g$  factor.

The temporal decay of the TRKR signal directly reflects the electron spin relaxation. The corresponding spin-relaxation time  $\tau_s$  was determined from exponential decay fits of the form  $[A_1 \exp(-t/\tau_c)+A_2]\exp(-t/\tau_s)$  to the zero-

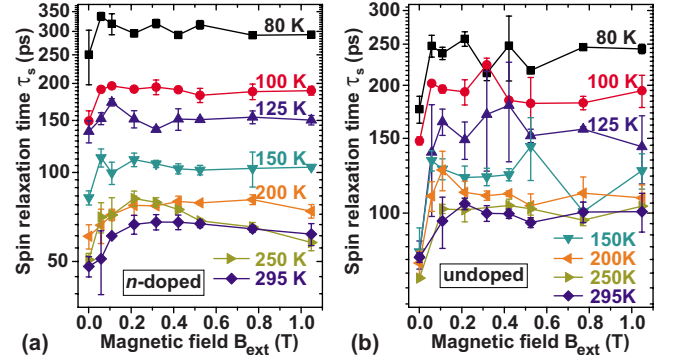


FIG. 3. (Color online) Temperature and magnetic field dependence of the spin-relaxation time  $\tau_s$  from 80 K up to 295 K and magnetic fields up to 1.05 T for (a) sample A and (b) sample B.

field ( $B_{\text{ext}}=0$ ) transients and from damped cosine fits  $[A_1 \exp(-t/\tau_c)+A_2]\exp(-t/\tau_s)\cos[\omega_L(t-t_0)]$  to the transients for  $B_{\text{ext}}>0$ , respectively.<sup>20</sup> The inclusion of the extra term  $A_1 \exp(-t/\tau_c)$  in the amplitude of the fits is necessary to account for the fast initial decay of carriers and to fit the TRKR transients over the whole time range [cf. Fig. 2(c)]. The carrier decay time  $\tau_c$  thus obtained agrees very well with the ones obtained from the fits to the TRR transients. Linear fits to the dependence of  $\omega_L$  on  $B_{\text{ext}}$  [cf. Eq. (1)] for each temperature give the Landé  $g$  factor. Its value of  $g=1.95 \pm 0.03$  for both samples in the whole temperature range is in good agreement with literature values<sup>21–23</sup> for the electron  $g$  factor, thus also demonstrating that the TRKR signal at times later than  $t \approx 50$  ps is solely due to electrons.

The temperature and magnetic field dependence of the spin-relaxation time  $\tau_s$  is shown in Figs. 3(a) and 3(b) for both samples at temperatures from 80 to 295 K and magnetic fields  $B_{\text{ext}}$  up to 1.05 T. Qualitatively,  $\tau_s$  follows in both samples the same dependence that is characterized by two main features: for fixed magnetic fields,  $\tau_s$  decreases monotonically with increasing temperature and for a fixed temperature,  $\tau_s$  increases significantly if an external magnetic field  $B_{\text{ext}}$  is applied.

In the following, we will show that this temperature and magnetic field dependence of  $\tau_s$  can be well explained by the D'yakonov-Perel' theory of spin relaxation. Basis for the D'yakonov-Perel' mechanism is the SOC-induced spin splitting of the conduction band. Scattering changes  $\mathbf{k}$  and accordingly  $\mathbf{\Omega}(\mathbf{k})$  randomly, forcing the electron's spin to precess around a randomly changing axis  $\mathbf{\Omega}(\mathbf{k})$ , thus dephasing the spin for an ensemble of electrons. In semiconductors with wurtzite structure, there are two contributions to the conduction-band spin splitting, one being linear in the electrons' wave vector  $k$  while the other one is proportional to the cube  $k^3$ .<sup>24</sup> The  $k^3$  dependent so-called Dresselhaus term<sup>25</sup> is also well known from semiconductors with zinc-blende structure and is a consequence of the bulk inversion asymmetry (BIA) of the crystal lattice. The  $k$ -linear contribution arises in the wurtzite structure due to the hexagonal symmetry<sup>26</sup> and reflects an intrinsic wurtzite structure inversion asymmetry (WSIA).<sup>27</sup> In analogy to the  $k$ -linear spin splitting in asymmetric two-dimensional (2D) zinc-blende structures, the WSIA-induced spin splitting is often also called Rashba effect.<sup>28</sup>

To calculate D'yakonov-Perel' spin-relaxation times for bulk semiconductors with wurtzite structure, we start with the Hamiltonian for both Dresselhaus<sup>29</sup> and Rashba<sup>26,28,30,31</sup> contributions

$$H_{so} = H_{so}^D + H_{so}^R = \frac{\hbar}{2} \mathbf{\Omega}(\mathbf{k}) \cdot \boldsymbol{\sigma} \quad (2)$$

with

$$\mathbf{\Omega}(\mathbf{k}) = \frac{2}{\hbar} \begin{pmatrix} [\gamma_e(bk_z^2 - k_{\parallel}^2) + \alpha_e]k_y \\ -[\gamma_e(bk_z^2 - k_{\parallel}^2) + \alpha_e]k_x \\ 0 \end{pmatrix}, \quad (3)$$

where  $z_{\parallel}[0001]$  ( $c$  axis),  $x_{\parallel}[1\bar{1}\bar{2}0]$ ,  $y_{\parallel}[1\bar{1}00]$  [cf. Fig. 4(a)],  $k_{\parallel}^2 = k_x^2 + k_y^2$ , and  $\boldsymbol{\sigma}$  is the vector of the Pauli spin matrices  $\sigma_i$ ,  $i=x, y, z$ . The Dresselhaus contribution is determined by the SOC parameters  $\gamma_e$  and  $b$ , the strength of the Rashba contribution is given by the Rashba coefficient  $\alpha_e$ . Figure 4(b) shows  $\mathbf{\Omega}(k_x, k_y, k_z)$  for  $k_z=0.1 \text{ \AA}^{-1}$  for the values of  $b$ ,  $\gamma_e$ , and  $\alpha_e$  listed in Table I, illustrating that  $\mathbf{\Omega}(\mathbf{k})$  always lies in the  $k_x$ - $k_y$ -plane and is perpendicular to  $\mathbf{k}$ .

The spin-relaxation dynamics in the absence of an external magnetic field is given by the equation of motion  $\dot{s}_i = -\sum_j \gamma_{ij} s_j$ , where  $\gamma_{ij}$  denotes the tensor of spin-relaxation rates and  $s_i$  the average spin component in direction  $i$ . In the most simplistic form of the D'yakonov-Perel' formalism,<sup>4</sup>  $\gamma_{ij}$  is determined by<sup>33,34</sup>

$$\gamma_{ij} = \frac{1}{2} (\delta_{ij} \langle \mathbf{\Omega}^2 \rangle - \langle \Omega_i \Omega_j \rangle) \tau_p, \quad (4)$$

where  $\tau_p$  is the momentum scattering time and  $\langle \dots \rangle$  denotes averaging over the momentum distribution of electrons. From Eq. (4) follows directly the anisotropy<sup>13,31</sup> of electron spin relaxation in bulk GaN that reveals itself in the sudden increase in the spin-relaxation time from the zero-field value  $\tau_s^0 = 1/\gamma_{zz}$  to  $4/3\tau_s^0$  for  $B_{\text{ext}} > 0$ , as is described in Ref. 13. This anisotropy of the spin relaxation persists at all temperatures, as can be seen from the magnetic field dependence of the spin-relaxation time in Fig. 3.

An external magnetic field can also additionally influence D'yakonov-Perel' relaxation directly via three mechanisms. (i) The Larmor precession around a sufficiently strong external magnetic field suppresses the precession around the random internal effective magnetic field, thus leading to a suppression of D'yakonov-Perel' relaxation.<sup>4,35</sup> (ii) In an external magnetic field, the orbital motion of electrons also influences the spin dynamics. The longitudinal component (along the external magnetic field) of the electron's quasimomentum is conserved while the orthogonal components precess around  $B_{\text{ext}}$  with the cyclotron frequency  $\omega_c$ . This precession leads to an averaging of the perpendicular components and thus to a weakening of D'yakonov-Perel' relaxation.<sup>36</sup> (iii) In contrast to the slow down of spin relaxation due to Larmor precession and the orbital motion, an external magnetic field can also enhance spin relaxation via the momentum dependence of the  $g$  factor.<sup>37,38</sup>

However, all three effects play a significant role only for high magnetic fields. As an estimate, the first two mecha-

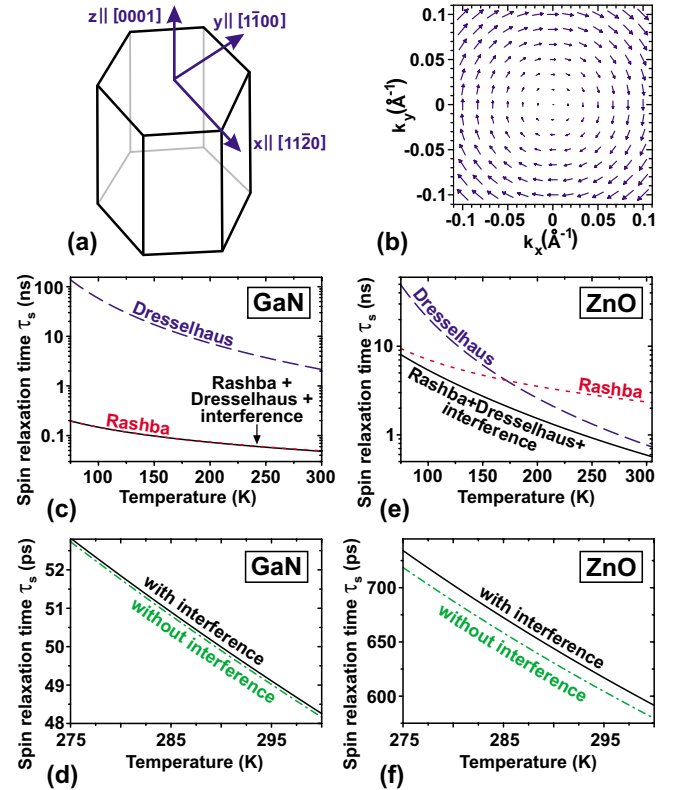


FIG. 4. (Color online) (a) Schematic unit cell of GaN and coordinate system used in the text. (b) Effective magnetic field  $\mathbf{\Omega}(k_x, k_y, k_z)$  for fixed  $k_z=0.1 \text{ \AA}^{-1}$ . The dimensions of the arrows are proportional to  $|\mathbf{\Omega}|$ . (c) Temperature dependence of the spin-relaxation time  $\tau_s^0$  calculated according to Eq. (5) for only the Rashba contribution (dotted red line), to Eq. (6) for only the Dresselhaus contribution (dashed blue line) and according to Eq. (8) for both contributions including the interference term (solid black line), for a scattering time  $\tau_p=40$  fs. (d) Comparison of the calculated spin-relaxation time for both Rashba and Dresselhaus contributions with (black line) and without (dashed-dotted green line) the interference term for temperatures from 275 to 300 K. (e) Calculated spin-relaxation time in ZnO for comparison with GaN, showing the spin-relaxation time for both Rashba and Dresselhaus contributions including their interference (solid black line), for only the Rashba contribution (dotted red line) and for only the Dresselhaus contribution (dashed blue line). (f) Comparison of the calculated spin-relaxation time in ZnO for both Rashba and Dresselhaus contributions with (black line) and without (dashed-dotted green line) the interference term.

nisms become important for magnetic fields where  $\omega_L \tau_p \gg 1$  and  $\omega_c \tau_p \gg 1$ ,<sup>4,31</sup> whereas for the magnetic field range  $B_{\text{ext}} \leq 1$  T used in the experiments,  $\omega_L \tau_p \ll 1$  and  $\omega_c \tau_p \ll 1$ . The additional spin-relaxation process via the momentum dependence of the  $g$  factor is also expected to be very weak for fields  $B_{\text{ext}} \leq 1$  T.<sup>38</sup> Thus, the constant, magnetic field independent experimental values of the spin-relaxation time for  $B_{\text{ext}} > 0$  are also in agreement with D'yakonov-Perel' theory.

As the central result, the temperature dependence of the spin-relaxation time will be discussed in the following. Therefore, we evaluate Eq. (4) assuming a Boltzmann distribution for the electron momentum, an isotropic effective electron mass  $m^*$  and neglecting the  $k$  dependence of  $b$ . Con-

TABLE I. Dresselhaus coefficient  $\gamma_e$  (in eV  $\text{\AA}^3$ ), parameter  $b$ , and Rashba coefficient  $\alpha_e$  (in eV  $\text{\AA}$ ) for wurtzite GaN and ZnO.

	$\gamma_e$	$b$	$\alpha_e$
GaN	0.33 <sup>a</sup>	3.959 <sup>a</sup>	9.0 <sup>b</sup>
ZnO	0.32 <sup>a</sup>	3.855 <sup>a</sup>	1.1 <sup>c</sup>

<sup>a</sup>From Ref. 24.

<sup>b</sup>From Ref. 32.

<sup>c</sup>From Ref. 26.

sidering first only the Rashba contribution, one obtains from Eq. (4) the spin-relaxation rate  $\gamma_{zz}^R$

$$\gamma_{zz}^R = \frac{4\alpha_e^2 m^* k_B T}{\hbar^4} \tau_p. \quad (5)$$

Taking into account only the Dresselhaus term, the relaxation rate  $\gamma_{zz}^D$

$$\gamma_{zz}^D = \frac{4(24 - 8b + 3b^2)\gamma_e^2 (k_B T)^3 m^{*3}}{\hbar^8} \tau_p \quad (6)$$

follows. For both Rashba and Dresselhaus contributions simultaneously, evaluation of Eq. (4) gives

$$\gamma_{zz} = \frac{4k_B T m^*}{\hbar^8} \{ [\alpha_e \hbar^2 + (b-4)\gamma_e m^* k_B T]^2 + (2b^2 + 8)\gamma_e^2 m^{*2} (k_B T)^2 \} \tau_p \quad (7)$$

$$= \gamma_{zz}^R + \gamma_{zz}^D + \gamma_{zz}^{int}, \quad (8)$$

where the interference of BIA and WSIA leads to an extra term

$$\gamma_{zz}^{int} = [8\alpha_e \gamma_e (b-4) m^{*2} (k_B T)^2] \tau_p / \hbar^6 \quad (9)$$

in addition to the mere sum of  $\gamma_{zz}^R$  and  $\gamma_{zz}^D$ . This interference term has been neglected for wurtzite structures so far,<sup>39,40</sup> though being well known from asymmetric 2D zinc-blende structures.<sup>5</sup> The relative importance of BIA and WSIA in GaN can be seen in Fig. 4(c), where the temperature-dependent spin-relaxation times  $\tau_s^0 = \gamma_{zz}^{-1}$  for zero magnetic field calculated according to Eq. (7) with the values of  $\gamma_e$ ,  $b$ , and  $\alpha_e$  given in Table I, an effective electron mass  $m^* = 0.2m_e$ ,<sup>41</sup> and  $\tau_p = 40$  fs are plotted. Comparing Dresselhaus [dashed blue line in Fig. 4(c)] and Rashba [dotted red line in Fig. 4(c)] contributions, it becomes obvious that D'yakonov-Perel' relaxation in GaN is almost completely governed by the Rashba term. Also the interference term gives only a very small correction as is shown by Fig. 4(d), since its value of  $b = 3.959$  makes the factor  $(b-4)$  in Eq. (9) small. For comparison, the temperature dependence of the spin-relaxation time in ZnO as an other wide-gap semiconductor with wurtzite structure is shown in Fig. 4(e). The temperature dependence is calculated according to Eq. (7), using the values of  $\gamma_e$ ,  $b$ , and  $\alpha_e$  given in Table I, an effective electron mass  $m^* = 0.28m_e$ ,<sup>42</sup> and  $\tau_p = 40$  fs. In ZnO, the relative importance of Dresselhaus and Rashba contributions is different from GaN: only for low temperatures the Rashba

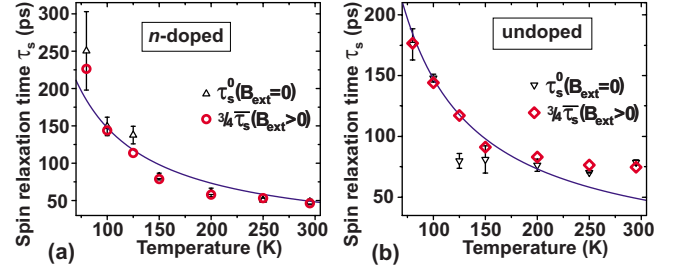


FIG. 5. (Color online) Temperature dependence of the spin-relaxation time  $\tau_s^0$  for  $B_{\text{ext}}=0$  (black triangles) and the averaged value  $3/4\bar{\tau}_s$  for  $B_{\text{ext}}>0$  (red circles and red diamonds, respectively) for (a) sample A and (b) sample B. The lines show spin-relaxation times calculated according to Eq. (7) for a scattering time  $\tau_p = 40$  fs.

term is dominating, while for temperatures  $>175$  K the Dresselhaus term governs the spin relaxation due to the occupancy of higher  $k$  states. The contribution from the interference term is larger in ZnO [cf. Fig. 4(f)].

The temperature dependence of spin relaxation according to Eq. (7) is compared to the experimental data in Fig. 5.<sup>43</sup> Since the zero-field values  $\tau_s^0$  [black triangles in Fig. 5] extracted from exponential decay fits to the TRKR transients are susceptible to drifts during the measurements, we plot in Fig. 5 as a more robust quantity also the average values<sup>44</sup> from the measurements with magnetic field [red circles and diamonds, respectively, in Fig. 5]. According to the above discussion of the magnetic field dependence of spin relaxation,  $3/4\bar{\tau}_s$  with  $\bar{\tau}_s$  as the average value of the spin-relaxation times for  $B_{\text{ext}}>0$  corresponds to the zero-field value  $\tau_s^0$ . The solid blue lines in Fig. 5 show the temperature-dependent spin-relaxation time  $\tau_s^0$  calculated according to Eq. (7) for zero magnetic field, assuming a temperature-independent momentum scattering time  $\tau_p = 40$  fs. The corresponding mobility  $\mu = \tau_p e / m^* \approx 350$  cm<sup>2</sup>/Vs is in the typical range of mobilities in similar GaN layers.<sup>17</sup> The good agreement of the calculated spin-relaxation times with the experimental results clearly demonstrates that electron spin relaxation for temperatures  $>80$  K is governed by the D'yakonov-Perel' mechanism. The small deviations between the experimental and theoretical values can be explained by the temperature dependence of the different scattering mechanisms: the electron-electron scattering rate is temperature dependent whereas electron-impurity scattering shows a much weaker temperature dependence. As was shown theoretically by Jiang and Wu,<sup>45</sup> the electron-electron scattering rate is close to the electron-impurity scattering rate for  $n$ -doped semiconductors in the nondegenerate regime while in undoped semiconductors the electron-electron scattering is even more important. Therefore, our assumption of a constant, temperature-independent scattering time gives better agreement for the doped sample. Despite the strong electron-longitudinal-optical phonon (LO) interaction in GaN, the above-mentioned effects are not masked by electron-LO phonon scattering because of the large LO phonon energy of 90 meV.<sup>46,47</sup>

In conclusion, the electron spin relaxation in  $n$ -type bulk

wurtzite GaN was investigated for temperatures from 80 to 295 K and external magnetic fields up to 1.05 T. The monotonic decrease in the spin-relaxation time  $\tau_s$  with increasing temperature is well reproduced by D'yakonov-Perel' relaxation theory. The magnetic field dependence shows for all temperatures a strong increase in  $\tau_s$  in an external magnetic field as a consequence of anisotropic D'yakonov-Perel' relaxation.

We gratefully acknowledge financial support by the German Science Foundation (DFG priority program 1285 "Semiconductor Spintronics") and thank the German-French University DFH/UFA for financial support under Grant No. CDFA-05-06 and A. D. Wieck and B. Vinter for its organization. J.H.B. was supported by the Ruhr-University Research School funded by Germany's Excellence Initiative (Grant No. DFG GSC 98/1).

- <sup>1</sup>*Spin Physics in Semiconductors*, edited by M. I. Dyakonov (Springer, New York, 2008).
- <sup>2</sup>*Semiconductor Spintronics and Quantum Computation*, edited by D. D. Awschalom, D. Loss, and N. Samarth (Springer, New York, 2002).
- <sup>3</sup>I. Žutić, J. Fabian, and S. Das Sarma, *Rev. Mod. Phys.* **76**, 323 (2004).
- <sup>4</sup>*Optical Orientation*, edited by F. Meier and B. P. Zakharchenya (North-Holland, Amsterdam, 1984).
- <sup>5</sup>R. Winkler, *Spin-Orbit Coupling Effects in Two-Dimensional Electron and Hole Systems* (Springer, New York, 2003).
- <sup>6</sup>H. Morkoç and S. N. Mohammad, *Science* **267**, 51 (1995).
- <sup>7</sup>F. A. Ponce and D. P. Bour, *Nature (London)* **386**, 351 (1997).
- <sup>8</sup>U. K. Mishra, L. Shen, T. E. Kazior, and Y.-F. Wu, *Proc. IEEE* **96**, 287 (2008).
- <sup>9</sup>T. Dietl, H. Ohno, F. Matsukura, J. Cibert, and D. Ferrand, *Science* **287**, 1019 (2000).
- <sup>10</sup>G. Bouzerar, T. Ziman, and J. Kudrnovský, *Europhys. Lett.* **69**, 812 (2005).
- <sup>11</sup>M. I. Dyakonov and V. I. Perel, *Sov. Phys. Solid State* **13**, 3023 (1972).
- <sup>12</sup>B. Beschoten, E. Johnston-Halperin, D. K. Young, M. Poggio, J. E. Grimaldi, S. Keller, S. P. DenBaars, U. K. Mishra, E. L. Hu, and D. D. Awschalom, *Phys. Rev. B* **63**, 121202(R) (2001).
- <sup>13</sup>J. H. Buß, J. Rudolph, F. Natali, F. Semond, and D. Hägele, *Appl. Phys. Lett.* **95**, 192107 (2009).
- <sup>14</sup>N. I. Zheludev, M. A. Brummell, R. T. Harley, A. Malinowski, S. V. Popov, D. E. Ashenford, and B. Lunn, *Solid State Commun.* **89**, 823 (1994).
- <sup>15</sup>R. T. Harley, O. Z. Karimov, and M. Henini, *J. Phys. D* **36**, 2198 (2003).
- <sup>16</sup>F. Semond, P. Lorenzini, N. Grandjean, and J. Massies, *Appl. Phys. Lett.* **78**, 335 (2001).
- <sup>17</sup>F. Semond, Y. Cordier, N. Grandjean, F. Natali, B. Damianno, S. Vézian, and J. Massies, *Phys. Status Solidi A* **188**, 501 (2001).
- <sup>18</sup>C. Brimont, M. Gallart, O. Crégut, B. Hönerlage, and P. Gilliot, *Phys. Rev. B* **77**, 125201 (2008).
- <sup>19</sup>T. Kuroda, T. Yabushita, T. Kosuge, A. Tackeuchi, K. Taniguchi, T. Chinone, and N. Horio, *Appl. Phys. Lett.* **85**, 3116 (2004).
- <sup>20</sup>The fits start at  $t=8$  ps when the coherent artifacts at zero time delay have vanished.
- <sup>21</sup>W. E. Carlos, J. A. Freitas, Jr., M. A. Khan, D. T. Olson, and J. N. Kuznia, *Phys. Rev. B* **48**, 17878 (1993).
- <sup>22</sup>A. V. Rodina and B. K. Meyer, *Phys. Rev. B* **64**, 245209 (2001).
- <sup>23</sup>W. F. Koehl, M. H. Wong, C. Poblentz, B. Swenson, U. K. Mishra, J. S. Speck, and D. D. Awschalom, *Appl. Phys. Lett.* **95**, 072110 (2009).
- <sup>24</sup>J. Y. Fu and M. W. Wu, *J. Appl. Phys.* **104**, 093712 (2008).
- <sup>25</sup>G. Dresselhaus, *Phys. Rev.* **100**, 580 (1955).
- <sup>26</sup>L. C. Lew Yan Voon, M. Willatzen, M. Cardona, and N. E. Christensen, *Phys. Rev. B* **53**, 10703 (1996).
- <sup>27</sup>I. Lo, W. T. Wang, M. H. Gau, S. F. Tsay, and J. C. Chiang, *Phys. Rev. B* **72**, 245329 (2005).
- <sup>28</sup>E. I. Rashba, *Sov. Phys. Solid State* **2**, 1109 (1960).
- <sup>29</sup>W.-T. Wang, C. L. Wu, S. F. Tsay, M. H. Gau, I. Lo, H. F. Kao, M.-E. Lee, Y.-C. Chang, C.-N. Chen, and H. C. Hsueh, *Appl. Phys. Lett.* **91**, 082110 (2007).
- <sup>30</sup>Y. A. Bychkov and E. I. Rashba, *JETP Lett.* **39**, 78 (1984).
- <sup>31</sup>A. D. Margulis and V. A. Margulis, *Sov. Phys. Semicond.* **18**, 305 (1984).
- <sup>32</sup>J. A. Majewski and P. Vogl, *Physics of Semiconductors: 27th International Conference on the Physics of Semiconductors*, edited by J. Menéndez and C. G. Van de Walle (American Institute of Physics, New York, 2005), p. 1403.
- <sup>33</sup>Here we corrected for a wrong sign between the  $\Omega$  terms, that appears in Eq. (35), page 90 in the often cited Ref. 4.
- <sup>34</sup>D. Hägele, S. Döhrmann, J. Rudolph, and M. Oestreich, *Adv. Solid State Phys.* **45**, 253 (2005).
- <sup>35</sup>M. I. Dyakonov and V. I. Perel, *Sov. Phys. JETP* **38**, 177 (1974).
- <sup>36</sup>E. L. Ivchenko, *Sov. Phys. Solid State* **15**, 1048 (1973).
- <sup>37</sup>A. D. Margulis and V. A. Margulis, *Sov. Phys. Solid State* **25**, 918 (1983).
- <sup>38</sup>F. X. Bronold, I. Martin, A. Saxena, and D. L. Smith, *Phys. Rev. B* **66**, 233206 (2002).
- <sup>39</sup>S. Ghosh, V. Sih, W. H. Lau, D. D. Awschalom, S.-Y. Bae, S. Wang, S. Vaidya, and G. Chapline, *Appl. Phys. Lett.* **86**, 232507 (2005).
- <sup>40</sup>N. J. Harmon, W. O. Putikka, and R. Joynt, *Phys. Rev. B* **79**, 115204 (2009).
- <sup>41</sup>I. Vurgaftman and J. R. Meyer, *J. Appl. Phys.* **94**, 3675 (2003).
- <sup>42</sup>E. Mollwo and R. Till, *Z. Phys.* **216**, 315 (1968).
- <sup>43</sup>The shorter values of  $\tau_s$  as compared to Ref. 13 are due to the different fitting procedure and local variations in  $\tau_s$  caused by sample inhomogeneities.
- <sup>44</sup>For the average, the values of  $\tau_s$  were weighted with their errors.
- <sup>45</sup>J. H. Jiang and M. W. Wu, *Phys. Rev. B* **79**, 125206 (2009).
- <sup>46</sup>R. Dingle, D. D. Sell, S. E. Stokowski, and M. Ilegems, *Phys. Rev. B* **4**, 1211 (1971).
- <sup>47</sup>J. D. Albrecht, R. P. Wang, P. P. Ruden, M. Farahmand, and K. F. Brennan, *J. Appl. Phys.* **83**, 4777 (1998).